Modelling of kinematic higher pairs by lower pairs

Meijaard, J. P.

DOI
10.1016/j.mechmachtheory.2023.105515

Publication date
2024

Document Version
Final published version

Published in
Mechanism and Machine Theory

Mechanism and Machine Theory 191 (2024) 105515

Contents lists available at ScienceDirect

Mechanism and Machine Theory

journal homepage: www.elsevier.com/locate/mechmt

Research paper

Modelling of kinematic higher pairs by lower pairs

J.P. Meijaard

Delft University of Technology, Faculty of Mechanical, Maritime and Materials Engineering, Department of Precision and Microsystems Engineering, Mekelweg 2, NL-2628 CD Delft, The Netherlands

ARTICLE INFO

Keywords:
Kinematic joints
Lower pairs
Higher pairs
Classification
Bicycle
Railway wheelset

ABSTRACT

Kinematic joints are classified in lower pairs and higher pairs. Most multibody modelling techniques focus on lower pairs, because a complete classification in six types is available. Higher pairs are more diverse. In this article, higher pairs that can be exactly modelled by lower pairs are investigated. A complete classification of higher pairs that can be modelled by a chain of five single-degree-of-freedom lower pairs with a central revolute joint at the contact point is proposed. Two-dimensional cases and surfaces with discontinuities are also considered. The equivalent chains can be used for exact and approximate modelling of higher pairs and as design alternatives. Illustrative examples and applications to a bicycle on toroidal wheels and a railway wheelset on a roller rig are shown.

1. Introduction

In the classification of kinematic joints, Reuleaux [1] has introduced the distinction between lower pairs, in which two bodies have conformal contact over a surface, and higher pairs, in which two bodies have line or point contact. The lower-pair joints have been completely classified into six types, namely the spherical joint, the planar joint, the cylindrical joint, the revolute joint, the prismatic joint and the screw joint, as shown in Fig. 1. On the other hand, higher pairs display a wide variety. Powerful analytic techniques for analysing mechanisms with only lower-pair joints have been developed [2–5] and the six lower-pair joints are available as standard modelling elements in most programs that deal with multibody system dynamics [6]. Some programs can model special classes of higher-pair joints, in particular the tyre–road contact of road vehicles, the wheel–rail contact of railway vehicles [7–9] and gears [10].

In general, it is not possible to model higher pairs with lower pairs except for some special cases. Planar cams with circular and tangent profiles actuating roller or flat-face followers have been modelled by lower pairs [11,12]. The modelling of the contact between two tori and its special cases has been presented [13]. In this article, the investigation into some classes of higher pairs whose kinematics can be modelled by a chain of lower pairs is continued. The purpose is to have an exact equivalence of the pairs, and not an approximation [14,15]. This equivalence shows that from a kinematic point of view, no sharp distinction can be made between lower pairs and higher pairs. The equivalent chains can be used for any mechanism, so equivalent mechanisms for specific cases will not be considered, which may serve a wider class of mechanisms with higher pairs, such as planar linkages with one degree of freedom, where moving and fixed centrodes have a rolling contact that can be used to replace a link [14].

The main motivation of the present study is in modelling multibody systems containing higher pairs. However, the results may be used to suggest alternative designs, as one may have more desirable properties than the other as to wear, friction or precision, and they may give a better understanding.

In the next section, a precise definition of the problem is formulated, restrictions are made and a classification is given. Then, some illustrative examples and applications to a bicycle and to a railway wheelset are presented.

E-mail address: j.p.meijaard@tudelft.nl.

https://doi.org/10.1016/j.mechmachtheory.2023.105515
Received 24 May 2023; Received in revised form 13 October 2023; Accepted 14 October 2023
Available online 25 October 2023

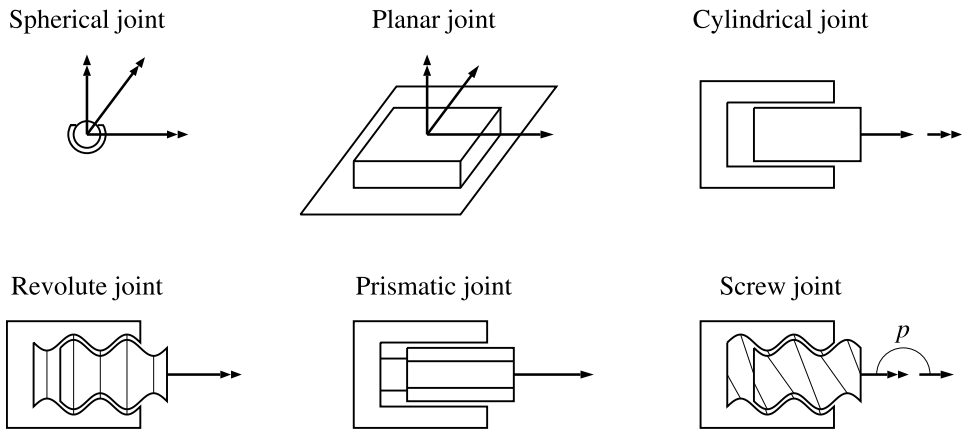

Fig. 1. Schematic drawing of the six types of lower-pair joints. The relative degrees of freedom are indicated by arrows for translations and double-headed arrows for rotations. The translation of the screw joint is related to its rotation by the pitch p.

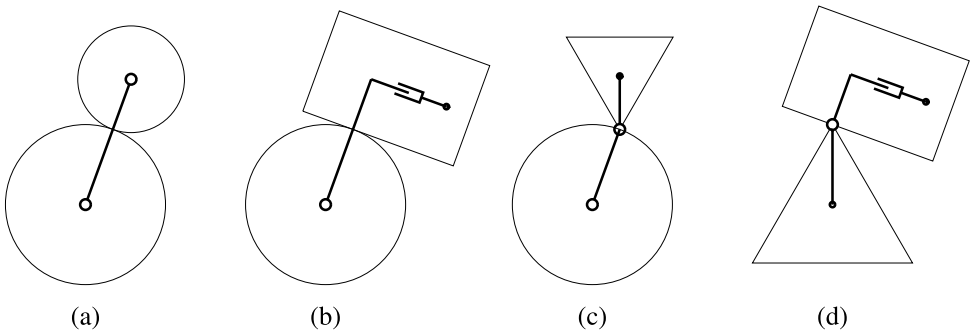

Fig. 2. Four kinds of planar higher pairs that can be modelled by lower pairs: (a) circle–circle, (b) circle–line, (c) circle–vertex and (d) line–vertex.

2. Classification of surfaces in contact that can be modelled by lower-pair joints

The kinds of higher pairs considered are two-dimensional pairs with line contact and spatial pairs with point contact. The two-dimensional pairs moving in a plane can consist of two smooth curves in contact or a smooth curve in contact with a vertex of another curve, which is a point with a discontinuity in the tangent. For the three-dimensional contact, the considered cases are the contact of two smooth surfaces, the contact of a smooth surface with a crest, the contact of a smooth surface with a vertex and the contact of two crests. A crest, or knife-edge, is here a smooth curve on a surface along which the normal vector of a surface has a jump discontinuity when the curve is transversally crossed and a vertex is a point with a discontinuous normal vector in all directions.

2.1. Two-dimensional contacts

A planar contact removes one in-plane degree of freedom, so the relative planar motion of the two contacting bodies has two degrees of freedom. This relative motion will be modelled by a serial chain with two joints with one degree of freedom, each of which describes a curve; these curves are in mutual contact. The curves that can be generated by planar lower-pair joints are a circle by a revolute joint and a line by a prismatic joint; the circle may degenerate into a point. The four cases are shown in Fig. 2, where it is seen that all basically consist of two circles in contact, where a circle may degenerate into a straight line, which is a circle with an infinite radius, or a vertex, which is a circle with a vanishing radius. The circles can have internal or external contact. The first three types can be used to model the contact between a circular cam and roller, flat-face and knife-edge followers. Other planar higher pairs might be generated by more involved mechanisms, which will not be investigated here.

2.2. Contact of two smooth surfaces

A class of higher pairs is considered in which two bodies with a smooth outer surface touch each other in a single point of contact. The contact condition reduces the dimension of the configuration space by one, and therefore the relative motion of the bodies can be described by five kinematic degrees of freedom. The kinematically equivalent mechanism with lower-pair joints is

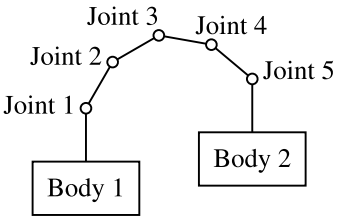

Fig. 3. Schematic representation of two bodies in contact interconnected by six links and five joints with one degree of freedom each; Joint 1 and Joint 2 generate the surface of Body 1, Joint 5 and Joint 4 generate the surface of Body 2 and Joint 3 is a revolute joint representing the rotation about the common normal at the contact point.

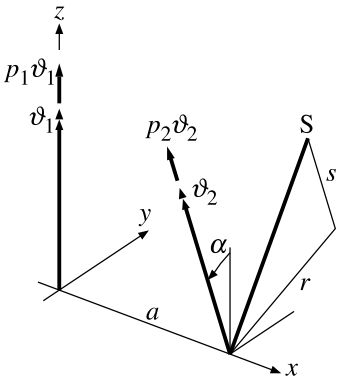

Fig. 4. Relative position of two screw joints in series with a representative point of a surface, S.

therefore chosen as a serial chain with five joints with a single degree of freedom each (Fig. 3). The two joints at either end of the chain with the three connected links describe the surface of a contacting body, whereas the central joint is a revolute joint with an axis of rotation through the contact point that is perpendicular to the common tangent plane of the contacting bodies, so it can describe the relative rotation about the common normal of these planes. This way of describing the contact of two bodies is comparable to the description of each surface by two parameters and imposing five constraints for the contact conditions as in the central revolute joint [16]. There might be equivalent lower-pair models for higher pairs that fall beyond this description, whose classification remains an open problem. The most general lower-pair joint with a single relative degree of freedom is the screw, which has as special cases the prismatic joint if the pitch is infinite and the revolute joint if the pitch is zero. A cylindrical joint can be seen as a prismatic joint and a revolute joint in series with a common axis.

Not all surfaces generated by arranging two lower-pair joints with one degree of freedom in series can be used to model higher pairs. The restriction is that the axis of the central revolute joint has to remain perpendicular to the generated surface. All possible combinations are being analysed next.

Firstly, the case of two general screws in series will be considered, where revolute joints appear as screws with a zero pitch. The first screw is placed between the body in contact and the second screw, whereas the second screw is placed between the first screw and the surface of the body (Fig. 4). Without loss of generality, the axis of the first screw can be placed along the global z-axis and the axis of the second screw in the reference configuration crosses the plane $z = 0$ at the point $x = a$, $y = 0$, where a is the shortest distance between the screw axes. The angle between the screw axes is denoted by α, which is the angle in the positive direction about the x-axis from the direction of the first screw axis to the direction of the second screw axis. The point on the surface in the reference configuration is assumed to be at the position

$$\mathbf{x}_0 = \begin{pmatrix} a \\ r\cos\alpha - s\sin\alpha \\ r\sin\alpha + s\cos\alpha \end{pmatrix}, \tag{1}$$

where r is the distance of the contact point to the second screw axis and s is the distance along the second screw axis form the plane $z = 0$ to the plane through the contact point perpendicular to the second screw axis in the reference configuration. The distance r must be positive in order to generate a surface. For a displaced configuration, the rotation angles of the screws are ϑ_1 and ϑ_2, whereas the pitches, expressed as a displacement per radian of rotation, are p_1 and p_2.

A rotation by ϑ_1 about the first screw axis can be represented by the rotation matrix

$$\mathbf{R}_{s1} = \begin{pmatrix} \cos\vartheta_1 & -\sin\vartheta_1 & 0 \\ \sin\vartheta_1 & \cos\vartheta_1 & 0 \\ 0 & 0 & 1 \end{pmatrix}. \tag{2}$$

The rotation from the first to the second screw axis by α and the rotation by ϑ_2 about the second screw axis in a local frame can be represented by the rotation matrices

$$\mathbf{R}_\alpha = \begin{pmatrix} 1 & 0 & 0 \\ 0 & \cos\alpha & -\sin\alpha \\ 0 & \sin\alpha & \cos\alpha \end{pmatrix}, \quad \mathbf{R}_{s2} = \begin{pmatrix} \cos\vartheta_2 & -\sin\vartheta_2 & 0 \\ \sin\vartheta_2 & \cos\vartheta_2 & 0 \\ 0 & 0 & 1 \end{pmatrix}. \tag{3}$$

The rotation matrix about the second screw axis expressed in the frame attached to the first screw is

$$\mathbf{R}_\alpha \mathbf{R}_{s2} \mathbf{R}_\alpha^{\mathrm{T}} = \begin{pmatrix} \cos\vartheta_2 & -\cos\alpha\sin\vartheta_2 & -\sin\alpha\sin\vartheta_2 \\ \cos\alpha\sin\vartheta_2 & \cos^2\alpha\cos\vartheta_2 + \sin^2\alpha & -\sin\alpha\cos\alpha(1-\cos\vartheta_2) \\ \sin\alpha\sin\vartheta_2 & -\sin\alpha\cos\alpha(1-\cos\vartheta_2) & \sin^2\alpha\cos\vartheta_2 + \cos^2\alpha \end{pmatrix}. \tag{4}$$

For $\vartheta_1 = 0$, the local frame follows from the global frame by a translation over a distance a along the global x-axis and a rotation over the angle α, and it moves with the first screw. The second screw motion displaces, in the local frame, the contact point from $(0, r, s)^{\mathrm{T}}$ to the point

$$\mathbf{x}' = \mathbf{R}_{s2} \begin{pmatrix} 0 \\ r \\ s \end{pmatrix} + \begin{pmatrix} 0 \\ 0 \\ p_2\vartheta_2 \end{pmatrix} = \begin{pmatrix} -r\sin\vartheta_2 \\ r\cos\vartheta_2 \\ s + p_2\vartheta_2 \end{pmatrix} = \begin{pmatrix} x' \\ y' \\ z' \end{pmatrix}. \tag{5}$$

In the frame rigidly attached to the first screw coinciding with the global frame for $\vartheta_1 = 0$, the coordinates are

$$\mathbf{x}'' = \mathbf{R}_\alpha \mathbf{x}' + \begin{pmatrix} a \\ 0 \\ 0 \end{pmatrix} = \begin{pmatrix} a - r\sin\vartheta_2 \\ r\cos\alpha\cos\vartheta_2 - (s + p_2\vartheta_2)\sin\alpha \\ r\sin\alpha\cos\vartheta_2 + (s + p_2\vartheta_2)\cos\alpha \end{pmatrix} = \begin{pmatrix} x'' \\ y'' \\ z'' \end{pmatrix}. \tag{6}$$

The first screw motion gives a translation of $p_1\vartheta_1$ in the direction of the z-axis and a rotation of ϑ_1 about the z-axis. The contact point in a general configuration therefore becomes

$$\mathbf{x} = \begin{pmatrix} x''\cos\vartheta_1 - y''\sin\vartheta_1 \\ x''\sin\vartheta_1 + y''\cos\vartheta_1 \\ p_1\vartheta_1 + z'' \end{pmatrix} = \begin{pmatrix} x \\ y \\ z \end{pmatrix}, \tag{7}$$

where x'', y'' and z'' have the values from Eq. (6). Tangent vectors to the surface of the body are now obtained as

$$\frac{\partial \mathbf{x}}{\partial \vartheta_1}(\vartheta_1, \vartheta_2) = \begin{pmatrix} -y \\ x \\ p_1 \end{pmatrix} = \mathbf{R}_{s1} \begin{pmatrix} -r\cos\alpha\cos\vartheta_2 + (s + p_2\vartheta_2)\sin\alpha \\ a - r\sin\vartheta_2 \\ p_1 \end{pmatrix} \tag{8}$$

and

$$\frac{\partial \mathbf{x}}{\partial \vartheta_2}(\vartheta_1, \vartheta_2) = \mathbf{R}_{s1} \begin{pmatrix} -r\cos\vartheta_2 \\ -r\cos\alpha\sin\vartheta_2 - p_2\sin\alpha \\ -r\sin\alpha\sin\vartheta_2 + p_2\cos\alpha \end{pmatrix} = \mathbf{R}_{s1}\mathbf{R}_\alpha\mathbf{R}_{s2} \begin{pmatrix} -r \\ 0 \\ p_2 \end{pmatrix}. \tag{9}$$

A normal vector can be found by taking the cross product of these two tangent vectors, except at singularities where the tangent vectors have the same direction.

The condition for the possibility of representing the higher-pair contact by the chosen series of lower-pair joints is now that the normal vector in some initial configuration remains a normal vector after a general displacement. The first screw motion transforms tangent vectors into tangent vectors and rotates the normal vector in the same way as the tangent vectors, so it remains orthogonal to the tangent vectors and the condition is fulfilled; therefore, only the case $\vartheta_1 = 0$, $\mathbf{R}_{s1}$ is the identity matrix, need be considered.

The second screw motion rotates the tangent vector $\partial\mathbf{x}/\partial\vartheta_2$ and the normal vector in the same way, so these vectors remain perpendicular in a general configuration. The tangent vectors are expressed in components in a local frame moving with the second screw, so the expressions in Eqs. (8) and (9) are premultiplied by $\mathbf{R}_{s2}^{\mathrm{T}}\mathbf{R}_\alpha^{\mathrm{T}}$, which yields

$$\mathbf{g}_1 = \begin{pmatrix} -r\cos\alpha + (p_1\sin\alpha + a\cos\alpha)\sin\vartheta_2 + (s + p_2\vartheta_2)\sin\alpha\cos\vartheta_2 \\ (p_1\sin\alpha + a\cos\alpha)\cos\vartheta_2 - (s + p_2\vartheta_2)\sin\alpha\sin\vartheta_2 \\ p_1\cos\alpha - a\sin\alpha + r\sin\alpha\sin\vartheta_2 \end{pmatrix} \tag{10}$$

and

$$\mathbf{g}_2 = \begin{pmatrix} -r \\ 0 \\ p_2 \end{pmatrix}, \tag{11}$$

where the tangent vectors in the local frame are denoted by $\mathbf{g}_1$ and $\mathbf{g}_2$. If the tangent vectors are not parallel, a normal vector corresponding to these vectors is

$$\mathbf{n} = \begin{pmatrix} p_2(p_1\sin\alpha + a\cos\alpha)\cos\vartheta_2 \\ -(p_1\cos\alpha - a\sin\alpha - p_2\cos\alpha)r - (r^2\sin\alpha + p_2(p_1\sin\alpha + a\cos\alpha))\sin\vartheta_2 \\ r(p_1\sin\alpha + a\cos\alpha)\cos\vartheta_2 \end{pmatrix} + (s + p_2\vartheta_2)\sin\alpha \begin{pmatrix} -p_2\sin\vartheta_2 \\ -p_2\cos\vartheta_2 \\ -r\sin\vartheta_2 \end{pmatrix}. \tag{12}$$

This normal vector must have a direction that is independent of the angle ϑ_2, that is, the cross product of $\mathbf{n}$ evaluated for some arbitrary value of ϑ_2 with $\mathbf{n}$ evaluated at some other arbitrary value of this angle, ϑ_2', must be the zero vector. Equivalently in the present case, the normal vector must be perpendicular to the tangent vector $\mathbf{g}_1$ for other arbitrary values, ϑ_2'. Because of the resulting products of secular terms, $p_2^3\vartheta_2\vartheta_2'\sin(\vartheta_2' - \vartheta_2)\sin^2\alpha$, this can only be the case if the secular terms disappear, that is, $p_2\sin\alpha = 0$. The case $p_2 = 0$, $\sin\alpha \neq 0$ leads to the conditions

$$p_2 = 0, \quad p_1\sin\alpha + a\cos\alpha = 0, \quad s = 0 \tag{13}$$

or the conditions

$$p_2 = 0, \quad p_1 = 0, \quad a = 0. \tag{14}$$

The case $\sin\alpha = 0$ (choose $\alpha = 0$, $\cos\alpha = 1$) leads to the conditions

$$\sin\alpha = 0, \quad a = 0 \tag{15}$$

or the conditions

$$\sin\alpha = 0, \quad p_1 = 0, \quad p_2 = 0. \tag{16}$$

Firstly, the case $\sin\alpha = 0$ is considered, in which the screw axes are parallel. If the conditions (15) are fulfilled, the screw axes coincide and the normal vector becomes

$$\mathbf{n} = \begin{pmatrix} 0 \\ -(p_1 - p_2)r \\ 0 \end{pmatrix}, \tag{17}$$

which is unequal to zero if the pitches are different. The resulting surface is a cylinder. Equal pitches do not yield a surface, but a helix. Either the first screw or the second screw can have a zero pitch, so one screw joint becomes a revolute joint.

If the conditions (16) are fulfilled, both joints are revolute joints with parallel axes, the normal vector becomes

$$\mathbf{n} = \begin{pmatrix} 0 \\ 0 \\ ra\cos\vartheta_2 \end{pmatrix}. \tag{18}$$

This case gives rise to a plane parallel to the xy-plane. At the boundaries of the reachable part of the plane, $\cos\vartheta_2 = 0$ and the normal vector is not unique.

Next, the case in which the second screw joint becomes a revolute joint and the axes have different directions is considered, $p_2 = 0$, $\sin\alpha \neq 0$. In the case of the conditions (13), $p_1 = -a\cos\alpha/\sin\alpha$ and the normal vector becomes

$$\mathbf{n} = \begin{pmatrix} 0 \\ ra/\sin\alpha - r^2\sin\alpha\sin\vartheta_2 \\ 0 \end{pmatrix}, \tag{19}$$

which may show singularities if $a \leq r\sin^2\alpha$. The condition $s = 0$ means that the contact point is in a plane perpendicular to the axis of the revolute joint through the point nearest to the first screw axis and the condition $p_1\sin\alpha + a\cos\alpha = 0$ means that the screw motion of the first joint moves this nearest point along a helix with the revolute joint axis tangent to this helix. The surface generated by this motion resembles the shape of a corkscrew with an open kernel if $r < a$ or a spiral column (Solomonic column). The parametric description of the surface is

$$\mathbf{x}(\vartheta_1, \vartheta_2) = \begin{pmatrix} (a - r\sin\theta_2)\cos\vartheta_1 - r\cos\alpha\cos\vartheta_2\sin\vartheta_1 \\ (a - r\sin\theta_2)\sin\vartheta_1 + r\cos\alpha\cos\vartheta_2\cos\vartheta_1 \\ p_1\vartheta_1 + r\sin\alpha\cos\vartheta_2 \end{pmatrix}. \tag{20}$$

If the first screw joint becomes a revolute joint too, we must have $a = 0$, the case of the conditions (14), giving rise to a spherical surface, or $\cos\alpha = 0$ with perpendicular axes giving rise to a torus.

If the second joint is a prismatic joint, the angle ϑ_2 has a fixed value and the translation along the axis, $s_2 = s$, is the new coordinate. As the axis may be positioned at an arbitrary place, we can choose $r = 0$. The tangent vectors are now

$$\frac{\partial\mathbf{x}}{\partial\vartheta_1}(0, s_2) = \begin{pmatrix} s_2\sin\alpha \\ a \\ p_1 \end{pmatrix}, \quad \frac{\partial\mathbf{x}}{\partial s_2}(0, s_2) = \begin{pmatrix} 0 \\ -\sin\alpha \\ \cos\alpha \end{pmatrix}. \tag{21}$$

Table 1
Surfaces generated by two joints with one degree of freedom and a normal vector transformed into normal vectors.

First joint	Second joint	Surface	Conditions
Prismatic	Prismatic	Plane	Non-parallel axes
Prismatic	Revolute	Cylinder Plane	Parallel axes Perpendicular axes
Prismatic	Screw	Cylinder	Parallel axes
Revolute	Prismatic	Cylinder Plane Cone	Parallel axes Perpendicular axes Oblique intersecting axes
Revolute	Revolute	Plane Sphere Torus	Parallel axes Intersecting axes Perpendicular axes
Revolute	Screw	Cylinder	Coincident axes
Screw	Prismatic	Cylinder Tangent surface	Parallel axes Prismatic joint axis, tangent to screw line
Screw	Revolute	Cylinder Spiral column	Coincident axes Revolute joint axis, tangent to screw line
Screw	Screw	Cylinder	Coincident axes, unequal pitch

The normal vector in the reference configuration with $s_2 = s$ is given by

$$\mathbf{n} = \begin{pmatrix} p_1 \sin\alpha + a\cos\alpha \\ -s\sin\alpha\cos\alpha \\ -s\sin^2\alpha \end{pmatrix}. \tag{22}$$

As this vector does not change due to a change in s_2 and should remain perpendicular to the first tangent vector, either $\sin\alpha = 0$ or $p_1\sin\alpha + a\cos\alpha = 0$. In the former case, the translation has the same direction as the screw axis and the resulting surface is a cylinder, which is independent of the pitch p_1. In the latter case, the axis of the prismatic joint is tangent to the screw motion at $s_2 = 0$. The parametric representation of the surface is

$$\mathbf{x}(\vartheta_1, s_2) = \begin{pmatrix} a\cos\vartheta_1 + s_2\sin\alpha\sin\vartheta_1 \\ a\sin\vartheta_1 - s_2\sin\alpha\cos\vartheta_1 \\ p_1\vartheta_1 + s_2\cos\alpha \end{pmatrix}. \tag{23}$$

This surface is a tangent surface, a developable ruled surface, to the helix generated by the screw motion for $s_2 = 0$. It has a cusp at $s_2 = 0$. If the surface is extended towards its self-intersection, it resembles a corkscrew with a closed kernel. In the case the first screw becomes a revolute joint, $p_1 = 0$, the axes of the joints are perpendicular and the surface becomes a plane and if additionally $a = 0$, the surface becomes a circular cone if the axes of the joints are neither parallel nor perpendicular.

Now we investigate the case in which the first screw becomes a prismatic joint. Its motion just adds a translation s_1 to the z-coordinate. The corresponding tangent vector is always $(0, 0, 1)^{\mathrm{T}}$. The condition on the normal vector is that it should always be in the xy-plane. This means that the second screw axis must be parallel to the axis of the prismatic joint, or it must be a revolute joint with an axis perpendicular to the axis of the prismatic joint, or it must be a prismatic joint. In the first case, the resulting surface is a cylinder, independent of the pitch p_2 and in the last two cases, the surface is a plane.

We can now make an overview of the different cases as shown in Table 1. Apparently, the surfaces that can be generated are a plane, a cylinder, a cone, a torus, a sphere, a spiral column and a tangent surface to a helix. The plane can be generated by two prismatic joints, a prismatic joint and a revolute joint with perpendicular axes, a revolute joint and a prismatic joint with perpendicular axes and two revolute joints with parallel axes. The cylinder can be generated by a prismatic joint and a revolute joint, or screw, with parallel axes, a revolute joint and a prismatic joint with parallel axes, a revolute joint and a screw with coinciding axes, a screw and a prismatic joint with parallel axes and a screw with another screw or revolute joint with coinciding axes if the pitches of the screws are different. A cone can be generated by a revolute joint and a prismatic joint with oblique intersecting axes. A sphere can be generated by two revolute joints with intersecting axes. A torus can be generated by two revolute joints with perpendicular non-intersecting axes. A screw and a prismatic joint can generate a tangent surface to a helix if the prismatic joint is tangent to this helix. A screw and a revolute joint can generate a spiral column if the axis of the revolute joint is tangent to a helix obtained from the screw motion.

Most pairs of the seven types of surface can be combined with the exceptions of a plane with another plane, which constitute a planar joint, and a plane with a cylinder, cone or tangent surface to a helix, which give rise to line contact. Furthermore, singular configurations or double contact may occur for finite relative motions, even if the initial configuration is non-singular with a single point of contact.

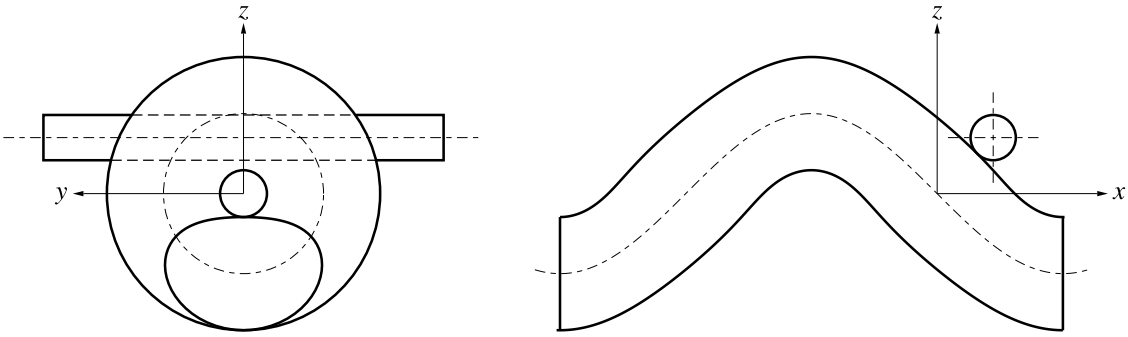

Fig. 5. Spiral column in contact with a cylinder with perpendicular axes.

For five types of surfaces, the equivalent chains are easy to find and mostly known. The cases of a spiral column and a tangent surface to a helix are not trivial and appear to have been unknown. There are no more surface contacts that can be modelled by a lower-pair kinematic chain with the proposed structure.

A displacement of the central joint parallel to its axis gives a chain with the same kinematics, which shows that each chain may model a one-parameter family of higher pairs, which are all equivalent. For a cylinder, sphere, torus and spiral column, this changes the radius or minor radius, whereas the plane, cone and tangent surface are displaced.

2.3. Special spatial cases

In the case that a surface is in contact with a crest, the surface can be modelled by any of the seven cases of the previous subsection, whereas the curve of the crest can be generated by a screw, with as special cases a revolute joint and a prismatic joint. The contact can be represented by two revolute joints with intersecting axes, where one axis is tangent to the curve and the other is perpendicular to the surface. A plane in contact with a line gives a line contact and has to be excluded. An example is a circular wheel with a knife-edge rim rolling on a plane.

In the case of a surface in contact with a vertex, the contact is modelled by a spherical joint and the surface can be any surface generated by any pair of revolute joints, screw joints and prismatic joints. The class of surfaces is therefore larger than in the case of contact between two smooth surfaces.

In the case of two crests in contact, any lines generated by a lower pair with one degree of freedom can be used. The contact is modelled by a spherical joint.

2.4. Slip velocities

The relative slip velocity, $\mathbf{s}$, at the contact point is determined by the joint velocities of the equivalent mechanism. It can be found by the equation

$$\mathbf{s} = \sum_{i=1}^{5} \left[\dot{\vartheta}_i (\mathbf{n}_i \times \mathbf{r}_{Ci} + p_i \mathbf{n}_i) + \dot{s}_i \mathbf{n}_i \right], \tag{24}$$

where $\dot{\vartheta}_i$ is the rotation rate of Joint i if it is a screw or revolute joint, $\dot{s}_i$ is the joint velocity if it is a prismatic joint; p_i is the pitch of a screw, $\mathbf{n}_i$ is the unit vector along the joint axis and $\mathbf{r}_{Ci}$ is the vector from a point on the joint axis to the contact point. Joint 3 has no contribution to the slip velocity vector. The normal component of the slip velocity vector, $\mathbf{s}^{\mathrm{T}}\mathbf{n}_3$, is zero due to the construction of the equivalent mechanism. The relative normal spin rate at the contact point, ψ, is given by

$$\psi = \sum_{i=1}^{5} \dot{\vartheta}_i \mathbf{n}_i^{\mathrm{T}} \mathbf{n}_3. \tag{25}$$

Conditions of a zero slip or normal spin, usually called non-holonomic constraints, can now be easily formulated with the equivalent mechanisms.

3. Examples of applications

3.1. Elementary examples

The motion of a cylinder in contact with a spiral column is considered. The spiral column has its axis along the global x-axis, with parameters normalized with the distance a, $p_1 = 1$, $a = 1$, $r = 0.5\sqrt{2}$. The cylinder has its axis parallel to the global y-axis and has a radius $r_c = 0.2\sqrt{2}$. The spiral column has a prescribed motion along the x-axis, whereas the cylinder is free to translate along

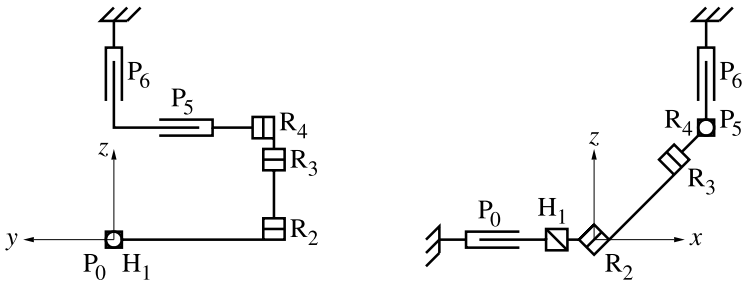

Fig. 6. Equivalent lower-pair chain (P: prismatic joint; H: screw joint; R: revolute joint); the prismatic joints P_0 and P_6 define the input and output motion, the other five joints model the higher pair.

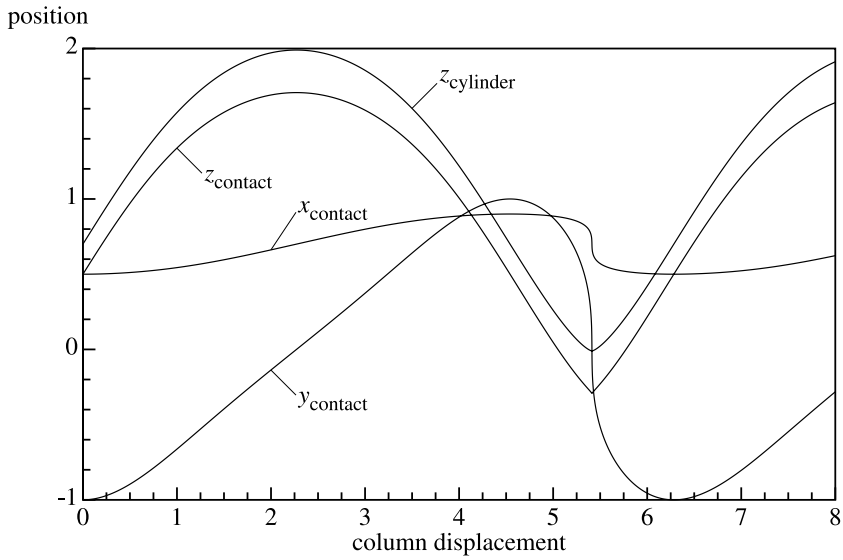

Fig. 7. Position of the contact point, $(x_{\text{contact}}, y_{\text{contact}}, z_{\text{contact}})$, and the vertical position of the cylinder, z_{cylinder}, for a spiral column in contact with a cylinder.

the global z-axis with a fixed value of 0.7 of the x-coordinate of its axis. In the initial configuration, shown in Fig. 5, the contact point has the coordinates $(0.5, -1.0, 0.5)^{\mathrm{T}}$. Fig. 6 shows the equivalent model with a prismatic joint P_0 for the input and a prismatic joint P_6 for the output motion. The joints H_1 and R_2 describe the surface of the spiral column and R_4 and P_5 describe the surface of the cylinder. Fig. 7 shows the position of the contact point and the z-coordinate of the centre line of the cylinder as functions of the x-displacement of the spiral column. At the lowest position of the cylinder at a column displacement of $3\pi/2 + 0.7 \approx 5.4124$, the x- and y-coordinates of the contact point moves very fast as is seen from the large value of the derivatives in the graph.

Next, the motion of a sphere in contact with a tangent surface of a helix is considered. The helix has its axis along the global z-axis and intersects the plane $z = 0$ in $x = a$, $y = 0$. The parameters normalized with the distance a are $p_1 = 1$, $a = 1$, and the radius of the sphere $r = 0.5\sqrt{2}$. Initially, the centre of the sphere is at $(1, 1.5, 2.5)^{\mathrm{T}}$, see Fig. 8. The equivalent kinematic model is shown in Fig. 9. The tangent surface can turn about the z-axis, indicated by the revolute joint R_0, and the sphere is constrained to move either along the y-axis or along the z-axis, the latter case being shown by the prismatic joint P_6 in the figure. The screw joint H_1 and the prismatic joint P_2 define the tangent surface and the revolute joints R_4 and R_5 define the sphere. If the sphere can move only along the z-axis, its displacement is proportional to the rotation angle with a coefficient equal to $-p_1$. If the sphere can move only in the y-direction, its displacement is proportional to the rotation angle with a coefficient equal to a.

3.2. Bicycle with toroidal wheels on plane surfaces

A basic bicycle model with wheels with toroidal tyres on plane surfaces is considered, as shown in Fig. 10 [17]. It consists of four rigid bodies: a frame, a front-fork assembly including the handlebar, and two wheels. These bodies are interconnected by three ideal revolute joints. The seven configuration coordinates are the coordinates of the rear wheel contact point in the plane surface, x_{r} and y_{r}, the yaw angle, ψ_{r}, the lean angle of the rear wheel, φ_{r}, the rear wheel pitch angle relative to the frame, χ_{rf}, the steering angle, β, and the pitch angle of the front wheel with respect to the front-fork assembly, χ_{ff}.

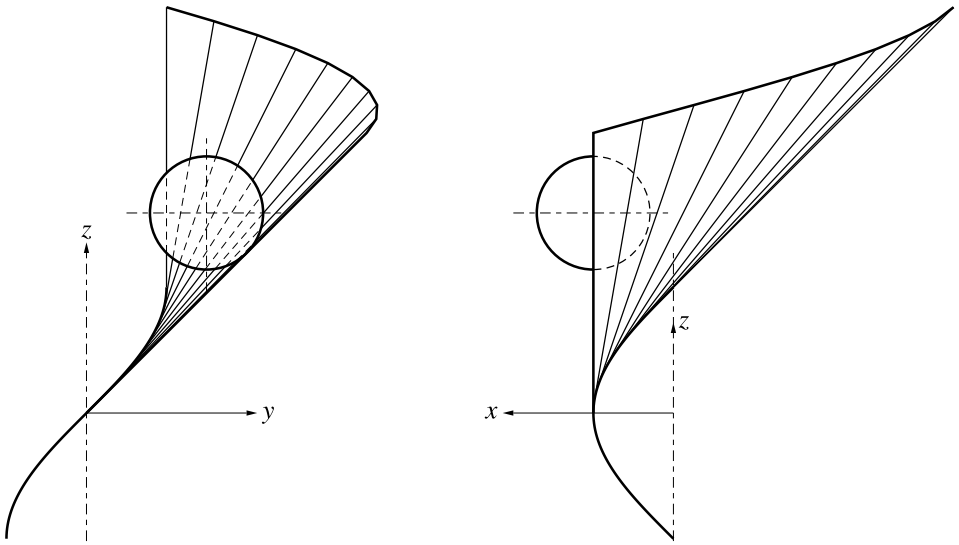

Fig. 8. Sphere in contact with a tangent surface to a helix with the part $0 \le \vartheta_1 \le \pi/2$, $s_2 \ge 0$ shown.

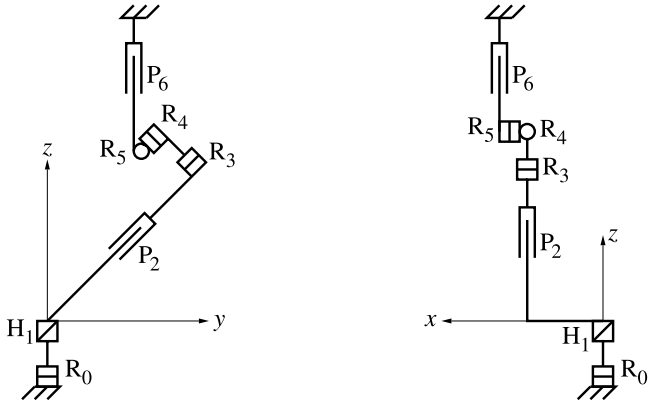

Fig. 9. Equivalent lower-pair chain (P: prismatic joint; H: screw joint; R: revolute joint); the revolute joint R_0 defines the input motion, the prismatic joint P_6 defines the output motion and the other five joints model the higher pair.

The kinematic structure of the bicycle with the equivalent mechanisms for the higher-pair contacts is shown in Fig. 11, in which misalignments of the joint axes of the wheel hubs and the steer are allowed for. Each of the two contacts is modelled by two prismatic joints for the contact point on the plane surface and a revolute joint for the yaw, which are combined in a planar joint, E_1 for the rear wheel and E_2 for the front wheel; the position and yaw angle at the front wheel contact point are described by the dependent coordinates x_f, y_f and ψ_f. The plane surface at the front wheel may differ from the surface at the rear wheel. The contact point at the rear wheel toroidal surface is described by the revolute joints R_1 and R_2 with perpendicular axes. Their joint angles are the roll angle φ_r and the wheel pitch angle χ_r. In the same way, the revolute joint R_7 models the dependent roll angle of the front wheel, φ_f, and the revolute joint R_6 models the dependent pitch angle of the front wheel, χ_f. The revolute joints R_3, R_4 and R_5 model the joint angles of the bicycle.

The equivalent mechanism can be used to formulate the equations for the dependent pitch angle of the frame of the bicycle, which can be shown to be reducible to a quartic. The procedure proposed by Hiller and Woernle [5] is used to derive this equation. A pair of joints in the closed loop is chosen and the loop closure conditions if one follows the loop along the two kinematic chains that connect the two chosen points are considered. In particular, conditions that are independent of the joint coordinates of the chosen pair are formulated. In the considered case, the two joints are chosen as E_2 and R_6 and the two conditions express that the z-coordinates of the position of joint R_6 if it is calculated from the two chains starting from E_2 is the same and that the projection of the joint axis of R_6 on the z-axis is the same. Only the rear wheel pitch angle χ_r and the front wheel roll angle φ_f appear as unknowns in these equations. These equations are linear in the sines and cosines of these unknown angles and can be written in

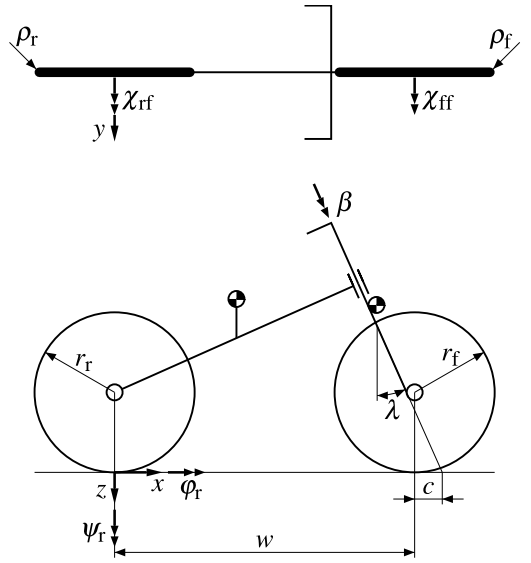

Fig. 10. Bicycle model with coordinates and main dimensions for the symmetric case with toroidal tyres and centred wheel hubs.

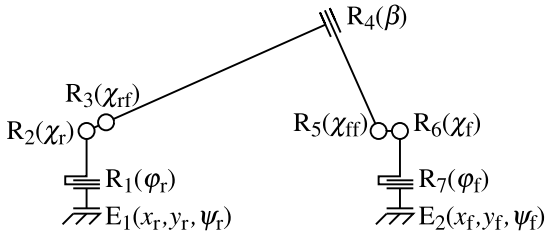

Fig. 11. Kinematic structure of the basic bicycle model.

the form

$$\begin{aligned} f(\chi_r) &= c_1 \sin\chi_r + c_2 \cos\chi_r + c_3 = \sin\varphi_f, \\ g(\chi_r) &= c_4 \sin\chi_r + c_5 \cos\chi_r + c_6 = \cos\varphi_f, \end{aligned} \tag{26}$$

where c_i $(i = 1, \ldots, 6)$ are coefficients depending on known quantities and the configuration coordinates. The roll angle of the front wheel, φ_f, can be eliminated, yielding the equation $f^2(\chi_r) + g^2(\chi_r) = 1$, together with the relation $\sin^2\chi_r + \cos^2\chi_r = 1$. These are two quadratic equations in the sine and cosine of the rear wheel pitch angle. With the substitutions

$$\sin\chi_r = \frac{2t}{1+t^2}, \quad \cos\chi_r = \frac{1-t^2}{1+t^2}, \tag{27}$$

where $t = \tan(\chi_r/2)$, the tangent of the half-angle, and multiplying out the denominators, a quartic in t is obtained in the form

$$a_0 t^4 + a_1 t^3 + a_2 t^2 + a_3 t + a_4 = 0, \tag{28}$$

where a_i $(i = 0, 1, 2, 3, 4)$ are coefficients that can easily be expressed in terms of the coefficients c_i in Eq. (26) as

$$\begin{aligned} a_0 &= (c_3 - c_2)^2 + (c_6 - c_5)^2 - 1, \\ a_1 &= 4c_1(c_3 - c_2) + 4c_4(c_6 - c_5), \\ a_2 &= 4(c_1^2 + c_4^2) + 2(c_3^2 - c_2^2 + c_6^2 - c_5^2 - 1), \\ a_3 &= 4c_1(c_2 + c_3) + 4c_4(c_5 + c_6), \\ a_4 &= (c_2 + c_3)^2 + (c_5 + c_6)^2 - 1. \end{aligned} \tag{29}$$

In a numerical solution of the quartic, the case a_0 equal or close to zero, which yields a solution for χ_r close to π, needs special attention. Using the cotangent instead of the tangent solves this singular case if a_4 is not close to zero. Otherwise, an arbitrary shift in the angle can be used.

Herewith it has been shown that the loop closure condition can be reduced to a quartic for the general case in which the wheels have toroidal tyre profiles and the three hinges connecting the parts are in a general position. This result expands the work by Psiaki [18] for a symmetric bicycle with knife-edge wheels and the work of Peterson and Hubbard [19] for a symmetric bicycle

with toroidal wheels. Psiaki formulated the contact conditions as a double root for the intersection of the circle representing the rim of the wheel and the ground plane. The quartic is not explicitly given, but can be easily derived from the given equation. Peterson and Hubbard formulated the quartic in the sine of the pitch angle, which may introduce spurious roots.

The case of a symmetric bicycle is worked out, in which the wheel hubs are located at the geometric centres of the toroidal wheels and their axes are perpendicular to the meridional plane of the wheel and to the steering axis. In this case, the hinges R_2 and R_3 are at the same place with the same orientation. Therefore, their rotation angles appear in the equations as their sum. A similar consideration is valid for the front wheel, where the hinges R_5 and R_6 are at the same place with the same orientation. The road surfaces of the rear and front wheels are the same. In the reference configuration, $\chi_r + \chi_{rf} = \chi_f + \chi_{ff} = \lambda$, the inclination angle of the steering axis.

The geometric parameters that determine the kinematic problem are the radius of the rear wheel, r_r, the transverse radius of the toroidal tyre at the rear wheel, ρ_r, the radius of the front wheel, r_f, the transverse radius of the toroidal tyre at the front wheel, ρ_r, the wheel base, w, the trail, c, and the inclination angle of the steering axis, λ. Auxiliary geometric parameters are the perpendicular distance of the rear-wheel axle to the steering axis, u_r, the perpendicular distance of the front-wheel axle to the steering axis, positive if the axle is in front of the steering axis, u_f, and the distance between these two perpendiculars, d,

$$\begin{aligned} u_r &= (w + c)\cos\lambda - r_r \sin\lambda,\\ u_f &= r_f \sin\lambda - c\cos\lambda,\\ d &= (r_r - r_f)\cos\lambda + w\sin\lambda. \end{aligned} \tag{30}$$

It should be noted that for this case, the joint coordinates of the planar joint E_1 and the rotation angles of the wheels do not appear in the loop closure equations; only the roll angle φ_r and the steering angle β appear. With the rotation matrices for roll, pitch and steer,

$$\begin{aligned} \mathbf{R}_\varphi &= \begin{bmatrix} 1 & 0 & 0\\ 0 & \cos\varphi_r & -\sin\varphi_r\\ 0 & \sin\varphi_r & \cos\varphi_r \end{bmatrix},\\ \mathbf{R}_\chi &= \begin{bmatrix} \cos(\chi_r + \chi_{rf}) & 0 & \sin(\chi_r + \chi_{rf})\\ 0 & 1 & 0\\ -\sin(\chi_r + \chi_{rf}) & 0 & \cos(\chi_r + \chi_{rf}) \end{bmatrix},\\ \mathbf{R}_\beta &= \begin{bmatrix} \cos\beta & -\sin\beta & 0\\ \sin\beta & \cos\beta & 0\\ 0 & 0 & 1 \end{bmatrix}, \end{aligned} \tag{31}$$

the z-component of the unit vector in the direction of the hinge axis of the revolute joint R_5 is the (3,2)-entry of the compound rotation matrix $\mathbf{R}_\varphi\mathbf{R}_\chi\mathbf{R}_\beta$,

$$\sin\varphi_r\cos\beta + \cos\varphi_r \sin(\chi_r + \chi_{rf})\sin\beta, \tag{32}$$

which must be equal to $\sin\varphi_f$. With subscript indices denoting a specific entry of a rotation matrix, the z-coordinate of the centre of the front wheel is

$$\begin{aligned} &-\rho_r - (r_r - \rho_r)(\mathbf{R}_\varphi)_{33} + u_r(\mathbf{R}_\varphi\mathbf{R}_\chi)_{31} + d(\mathbf{R}_\varphi\mathbf{R}_\chi)_{33} + u_f(\mathbf{R}_\varphi\mathbf{R}_\chi\mathbf{R}_\beta)_{31}\\ &\quad = -\rho_r - (r_r - \rho_r)\cos\varphi_r - u_r\cos\varphi_r\sin(\chi_r + \chi_{rf}) + d\cos\varphi_r\cos(\chi_r + \chi_{rf})\\ &\qquad + u_f\big(\sin\varphi_r\sin\beta - \cos\varphi_r\sin(\chi_r + \chi_{rf})\cos\beta\big), \end{aligned} \tag{33}$$

which must be equal to $-\rho_f - (r_f - \rho_f)\cos\varphi_f$. With these expressions, the coefficients in the two loop closure equations as in Eq. (26) with χ_r replaced by $\chi_r + \chi_{rf}$ are found to be

$$\begin{aligned} c_1 &= \cos\varphi_r\sin\beta,\\ c_2 &= 0,\\ c_3 &= \sin\varphi_r\cos\beta,\\ (r_f - \rho_f)c_4 &= u_r\cos\varphi_r + u_f\cos\varphi_r\cos\beta,\\ (r_f - \rho_f)c_5 &= -d\cos\varphi_r,\\ (r_f - \rho_f)c_6 &= -u_f\sin\varphi_r\sin\beta + \rho_r - \rho_f + (r_r - \rho_r)\cos\varphi_r. \end{aligned} \tag{34}$$

The coefficients in the quartic can be calculated according to Eq. (29), which can be analytically or numerically solved.

3.3. Railway wheelset on a roller rig

A final example considers the motion of a railway wheelset on a drum representing a roller rig [20]. The wheelset consists of an axle to which two wheels are rigidly connected so that it is rotationally and left–right symmetric, as shown in Fig. 12. The wheels have tyres with a hollow toroidal shape with a radius of curvature ρ_w; this radius becomes infinite for conical tyres. The drum has two toroidal contacting rings attached to its surface and it can rotate about its axis of symmetry. The radius of curvature of the rings is ρ_r. The longitudinal motion of the centre of the wheelset is suppressed as a constraint. In the reference configuration, the axes of the wheelset and the drum are parallel and the centre of the wheelset is right above the centre of the drum; furthermore,

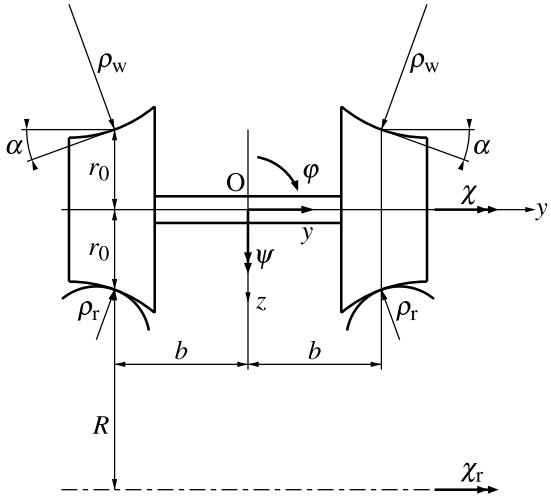

Fig. 12. Railway wheelset on a roller rig.

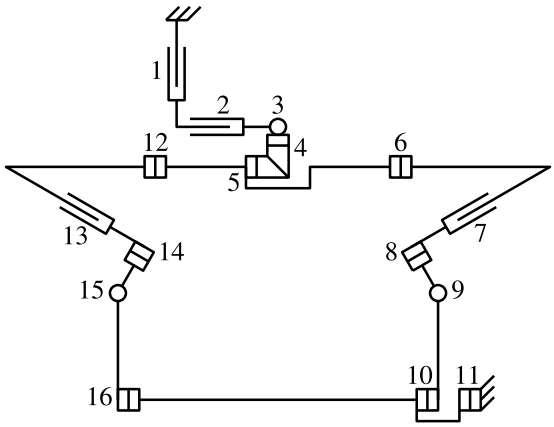

Fig. 13. Kinematic model of a railway wheelset with conical wheels on a roller rig with toroidal rings.

the contact points are located at a lateral distance b from the centre, where the radius of the wheels is r_0, the radius of the rings is R and the tangent plane makes an angle α with the axis of the wheelset.

A kinematic model for the case in which the wheels are conical is shown in Fig. 13. The prismatic joint 1 allows a vertical motion z of the centre of the wheelset and the prismatic joint 2 describes the lateral displacement y. The longitudinal displacement of the centre of the wheelset is suppressed. The revolute joint 3 describes the roll angle φ, the revolute joint 4 the yaw angle ψ and the revolute joint 5 the pitch angle χ. The contact point on the right-hand conical wheel is described by the revolute joint 6 and the prismatic joint 7, whereas the contact point on the right-hand ring of the drum is described by the revolute joints 10 and 9 and the relative normal rotation at the contact point by the revolute joint 8. The revolute joint 11 describes the rotation of the drum with the rotation angle χ_r. In a similar manner as the joints 6–10, the joints 12–16 describe the contact at the left-hand wheel. There are 16 joints with one joint coordinate each and two closed loops restricting six coordinates each, so the dimension of the configuration space is four. The coordinates to describe the configuration are chosen as y, ψ, χ and χ_r. The pitch angles leave the contact points fixed in space, so the joint coordinates of the other joints depend on the lateral displacement y and the yaw angle ψ.

For the special case in which only a lateral displacement is present, $\psi = 0$, the kinematics can be easily solved: the only coordinates that change their values are $y = s_2$, $z = s_1$, φ, s_7, θ_9, s_{13} and θ_{15} and the angles φ, θ_9 and θ_{15} have the same magnitude. Closed-form solutions for the dependent coordinates can be obtained for a tangent track [21]. If no-slip conditions at the contact points are fulfilled, three independent velocity-constraints are imposed and the system has a single dynamic degree of freedom.

4. Conclusions

The problem of finding higher-pair joints that can be modelled by lower-pair joints has been investigated. For the case the lower-pair joints form a chain of five single-degree-of-freedom joints in which the middle joint is a revolute joint at the contact

point modelling the relative rotation of the bodies around an axis normal to the contact surface, a classification of surfaces in contact that can be modelled by this chain has been made. The seven kinds of surfaces that allow such a representation are a plane, a cylinder, a cone, a torus, a sphere, a spiral column and a tangent surface to a helix. Two-dimensional higher pairs and contacts between surfaces with discontinuities appear as special cases. The existence of other classes of higher pairs that can be modelled by lower pair joints by different types of mechanisms remains a subject for further study.

The examples illustrate the usefulness of modelling higher pairs by kinematically equivalent lower pairs for obtaining analytic solutions and for modelling the systems with standard multibody dynamics software. A kinematic model of a bicycle with toroidal wheels on a flat ground showed that the equation for the pitch angle can be reduced to a quartic for a general asymmetric case. Also a railway vehicle with toroidal wheel profiles running on a straight track with cylindrical rails or on a roller rig with toroidal rings could be modelled.

Although analysis has been stressed, the results can also be used to suggest alternative designs for mechanisms containing higher pairs, or to enhance the understanding of mechanisms with higher pairs.

Declaration of competing interest

The authors declare that they have no known competing financial interests or personal relationships that could have appeared to influence the work reported in this paper.

Data availability

No data was used for the research described in the article.

References

[1] F. Reuleaux, Theoretische Kinematik; Grundzüge einer Theorie des Machinenwesens, Friedrich Vieweg und Sohn, Braunschweig, 1875.
[2] J. Angeles, Fundamentals of Robotic Mechanical Systems: Theory, Methods, and Algorithms, Springer, New York, 1997.
[3] C. Woernle, Ein systematisches Verfahren zur Aufstellung der geometrischen Schließbedingungen in kinematischen Schleifen mit Anwendung bei der Rückwärtstransformation für Industrieroboter, in: Fortschrittberichte VDI, Reihe 18, Nr. 59, VDI-Verlag, Düsseldorf, 1988.
[4] H. Li, Ein Verfahren zur Vollständigen Lösung der Rückwärtstransformation für Industrieroboter mit allgemeiner Geometrie (Dissertation), Universität-Gesamthochschule-Duisburg, Duisburg, 1990.
[5] M. Hiller, C. Woernle, A systematic approach for solving the inverse kinematic problem of robot manipulators, in: E. Bautista, J. Garcia-Lomas, A. Navarro, J. Dominguez, J. Nieto (Eds.), The Theory of Machines and Mechanisms, Proceedings of the 7th World Congress, 17–22 September 1987, Sevilla, Spain, Vol. 2, Pergamon Press, Oxford, 1987, pp. 1135–1139.
[6] W. Schiehlen (Ed.), Multibody Systems Handbook, Springer-Verlag, Heidelberg, 1990.
[7] W. Kortüm, R.S. Sharp (Eds.), Multibody computer codes in vehicle system dynamics, in: Vehicle System Dynamics Supplement, Vol. 22, 1993.
[8] S. Iwnicki, The Manchester benchmarks for rail vehicle simulation, in: Vehicle System Dynamics Supplement, Vol. 31, 1999.
[9] S. Bruni, J.P. Meijaard, G. Rill, A.L. Schwab, State-of-the-art and challenges of railway and road vehicle dynamics with multibody dynamics approaches, Multibody Syst. Dyn. 49 (2020) 1–32.
[10] A.L. Schwab, J.P. Meijaard, The belt, gear, bearing and hinge as special finite elements for kinematic and dynamic analysis of mechanisms and machines, in: T. Leinonen (Ed.), Proceedings of the Tenth World Congress on the Theory of Machines and Mechanisms, June 20–24, 1999, Vol. 4, University of Oulu, Oulu, 1999, pp. 1375–1386.
[11] M.F. Spotts, Straight line follower motions obtained with circular arc cams, Prod. Eng. 21 (1950) 110–114.
[12] H.A. Rothbart, Cams, Design, Dynamics and Accuracy, John Wiley and Sons, New York, 1956.
[13] T. Bil, Kinematic analysis of a universal spatial mechanism containing a higher pair based on tori, Mech. Mach. Theory 46 (2011) 412–424.
[14] R.S. Hartenberg, J. Denavit, Kinematic Synthesis of Linkages, McGraw-Hill, New York, 1964.
[15] W.-T. Chang, D.-Y. Yang, A note on equivalent linkages of direct-contact mechanisms, Robotics 9 (2020) 38, http://dx.doi.org/10.3390/robotics9020038.
[16] A.A. Shabana, J.R. Sany, An augmented formulation for mechanical systems with non-generalized coordinates: application to rigid body contact problems, Nonlinear Dynam. 24 (2001) 183–204.
[17] J.P. Meijaard, The loop closure equation for the pitch angle in bicycle kinematics, in: Proceedings, Bicycle and Motorcycle Dynamics 2013, Symposium on the Dynamics and Control of Single Track Vehicles, 11–13 November 2013, Narashino, Japan, 2013, p. 6.
[18] M.L. Psiaki, Bicycle Stability: A Mathematical and Numerical Analysis (B.A. thesis), Princeton University, Princeton NJ, 1979.
[19] D.L. Peterson, M. Hubbard, Analysis of the holonomic constraint in the Whipple bicycle model, in: M. Estivalet, P. Brisson (Eds.), The Engineering of Sport 7, Volume 2, Springer, Paris, 2008, pp. 623–631.
[20] J.P. Meijaard, The motion of a railway wheelset on a track or on a roller rig, in: P. Hagedorn, E. Clerkin (Eds.), IUTAM Symposium Analytical Methods in Nonlinear Dynamics, Frankfurt am Main, Germany, July 5–9, 2015, Procedia IUTAM 19, 2016, pp. 274–281.
[21] M. Antali, G. Stepan, S.J. Hogan, Kinematic oscillations of railway wheelsets, Multibody Syst. Dyn. 34 (2015) 259–274.